A FRACTAL IMAGE ANALYSIS METHODOLOGY FOR HEAT DAMAGE INSPECTION IN CARBON FIBER REINFORCED COMPOSITES

Aswin Haridas [a], Alexandru Crivoi [a], P. Prabhathan [a], Kelvin Chan [c] and V.M. Murukeshan *[b]

[a]Rolls-Royce@NTU Corporate Laboratory, 65 Nanyang Drive, Nanyang Technological University, Singapore 637460; [b]School of Mechanical and Aerospace Engineering, 50 Nanyang Drive, Nanyang Technological University, Singapore 639798; [c]Rolls-Royce Singapore, 6 Seletar Aerospace Rise, Singapore 797575

ABSTRACT

The use of carbon fiber-reinforced polymer (CFRP) composite materials in the aerospace industry have far improved the load carrying properties and the design flexibility of aircraft structures. A high strength to weight ratio, low thermal conductivity, and a low thermal expansion coefficient gives it an edge for applications demanding stringent loading conditions. Specifically, this paper focuses on the behavior of CFRP composites under stringent thermal loads.

The properties of composites are largely affected by external thermal loads, especially when the loads are beyond the glass temperature, Tg, of the composite. Beyond this, the composites are subject to prominent changes in mechanical and thermal properties which may further lead to material decomposition. Furthermore, thermal damage formation being chaotic, a strict dimension cannot be associated with the formed damage. In this context, this paper focuses on comparing multiple speckle image analysis algorithms to effectively characterize the formed thermal damages on the CFRP specimen. This would provide us with a fast method for quantifying the extent of heat damage in carbon composites, thus reducing the required time for inspection. The image analysis methods used for the comparison include fractal dimensional analysis of the formed speckle pattern and analysis of number and size of various connecting elements in the binary image.

Keywords: Image processing, Fractal dimension, Carbon Fiber Reinforced Plastics (CFRP), Thermal damage

1. INTRODUCTION

Non-destructive characterization of composite structures is a fundamental concern because of their widespread use in a variety of industries. High strength-to-weight ratio and stiffness-to-weight ratio combined with a high corrosion resistance and dimensional stability make it the right contender for load carrying aerospace structures [1]. Being one of the most capable structures in load carrying applications, it is quite essential to characterize its failure mechanism. This requires the development of non-destructive methodologies and sensors to play an effective role in defect detection, characterization, and analysis [2-3].

After the advent of lasers, optical methods have seen far-reaching applications in manufacturing and testing domains in a variety of engineering and biological domains employing both specular and speckle-based approaches [3-21]. Speckle-based optical techniques in non-destructive evaluation have acquired much attention due to its many advantages such as non-contact, large area and high-speed measuring capabilities. When a coherent beam of light is directed onto an optically rough surface, the scattered light interferes generating a speckle pattern [5-8]. Although speckles have been considered as a noise source in image capture, their grainy structure carries important properties of the underlying surface. Multiple researchers have shown the importance of accessing the statistical properties contained in a speckle pattern to extract meaningful about the surface quality [22-30]. On the other hand, researchers have also harnessed meaningful conclusions based on imaging speckle patterns varying with time to study processes involving movements of the speckle generating object. Applications such as corrosion detection and biological sample analysis being a few [23-34].

*mmurukeshan@ntu.edu.sg; Tel: +65 6790 4200; mae.ntu.edu.sg

International Conference on Optical and Photonics Engineering (icOPEN 2017), edited by Anand Krishna Asundi, Proc. of SPIE Vol. 10449, 104491L · © 2017 SPIE · CCC code: 0277-786X/17/$18 doi: 10.1117/12.2270727

However, no study has been extended to understand and utilize the change in speckle properties while non-destructively characterizing the extent of the damage. In this context, we propose a methodology to capture the speckle pattern variations due to thermal excitation of a thermally damaged composite panel. We analyze the transient variations in the observed speckle images with respect to the degree of thermal damage applied on the panel. We also develop speckle image processing algorithms based on fractal properties and element connectivities.

2. MATERIALS AND METHOD

In order to understand the variations of the speckle patterns with respect to the thermal damage in CFRP, we consider the following specimen shown in Fig. 1. The specimen is a 30×30 cm^2, ~0.2 cm thick CFRP composite panels with a 0^0 unidirectional lay, from SPORE HOBBY having a model number #2A-120612. These panels are then divided into 4 squares, each defined by an area of 15×15 cm^2. The material properties and the process of thermal loading are similar to what has been explored in the previous studies [34]. To prepare the specimen, each of the individual squares is thermally loaded with different temperature settings, using a heat gun, for a fixed heating time of 35 minutes.

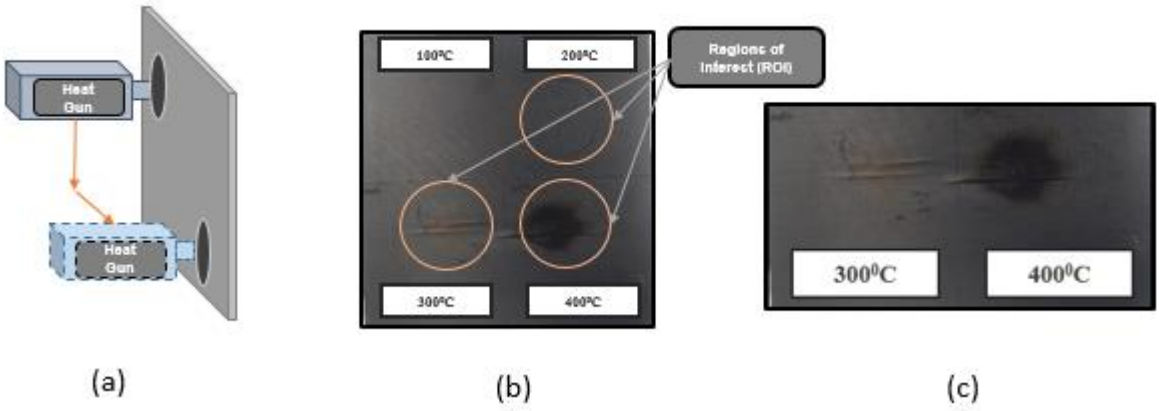

Fig.1 (a) The methodology used for producing the thermal damage using a heat gun, (b) final warped and damaged sample with the created heat damages and (c) shows the observable defect or cracks noticed for the location thermally excited by 300^0C and 400^0C.

It has been observed that the panels having been heated with multiple thermal loads show warpage due to varying thermal expansions. This particularly adds complexity to any optical methods chosen for inspection due to the variations in the angle of reflection due to the curvature.

Further, the experimental setup to understand the variations of the speckle pattern due to the formed damage is shown in Fig. 2.

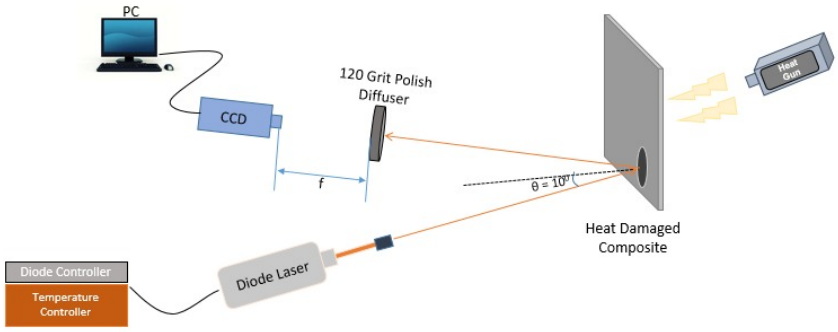

Fig.2 Experimental arrangement to measure the variations in the speckle patterns caused due to the surface variations and the subsurface defects of a heat damaged composite panels.

Here, we have used a laser diode (THORLABS L660P120) with an illumination wavelength of 660 nm with a maximum power of 120 mW controlled by a digital controller (LDC205C) and a temperature controller (TED200C). The expanded laser beam illuminates the region of interest having a radius of approximately 60 mm. The incident angle of illumination is 10^0. The reflected light is then passed through a diffuser (DGK01) with a polish of 120 grits. The CCD camera is then focused onto the diffuser to observe the speckle pattern variations from the specimen surface. In order to test the variation of the speckles with respect to the damaged area in focus (at the distance f), we apply an excitation load in the form of heat by a heat gun. With a heat exciting time of 30 seconds, we capture 10 images during the cooling cycle for the analysis of the speckle pattern. It has to be noted that the excitation zone is kept separate from the defect area in focus, this is to avoid unnecessary errors that could be added on because of the overall material expansion.

3. EXPERIMENTAL RESULTS AND DISCUSSION

This section details the results from processing the speckle images captured from the diffuser, which itself is illuminated by the reflection of the laser source from the inspection area on the composite sample. The first part of this section discusses the peculiarity of the obtained speckle images over time along the cooling process of the thermally excited specimen. Second, we shall use the captured framework of observed speckle variation in order to develop subsequent image processing algorithms for quantifying the extent of the damage. Third, we discuss and compare the outcomes of the different analysis methodologies to determine the best-suited algorithm to capture and quantify the damaged on the CFRP panel.

3.1 Speckle image variation over the damaged area during the cooling process after thermal excitation

To determine the adequate algorithm to be used for damage analysis, we compare the speckle images observed over a 3-second interval for a total of 30 seconds. Analysis of the obtained images based on differences in their binary equivalent would be used as a benchmark to select the image processing algorithm for characterization of the damage. In an alternate research using shearography and ultrasound to characterize these samples, it has been observed that the location damaged by a 100^0C heat load show no damage at all and thus, we do not incorporate the same in this study [24]. Fig. 1, shows the speckle images captured at 0 seconds for the (a) 200^0C, (b) 300^0C and (c) 400^0C damage locations, respectively.

For the effective characterization of the speckle image, it is important to analyze the image more clearly and closely. This is done by cropping the central zone for all the images, keeping the crop area and location the same for all it is observed that images are aligned covering the same sensor area on the CCD. Also, as the specimen used have a warpage generated due to the formed thermal damage, the images from different thermal damages show differences in luminosity. Thus, adequate image processing methods have been employed to ensure that the correct parameters are being compared.

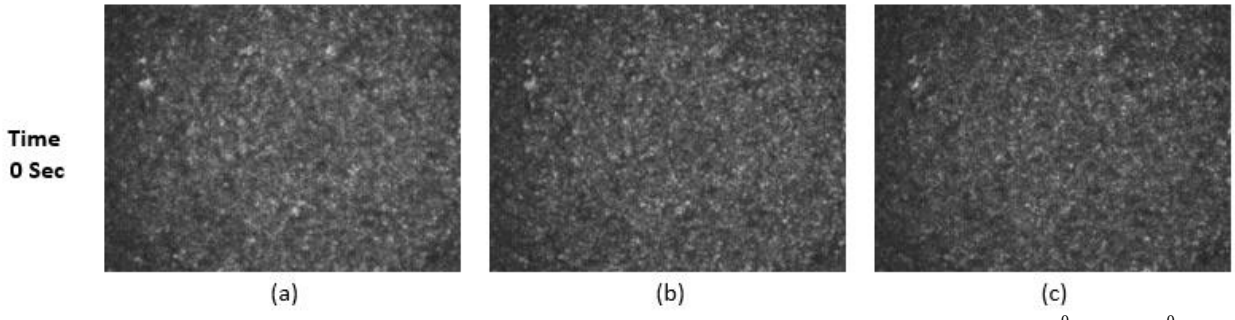

Fig.3 Speckle images captured from the diffuser at 0 seconds into the cooling down cycle of the CFRP at (a) 200^0C, (b) 300^0C and (c) 400^0C

Before distinguishing the speckle patterns observed at the locations of thermal damage, we also look at how the speckle pattern varies with cooling time. Thus, Fig. 4, describes the speckle images captured at 30 seconds for the (a) 200^0C, (b) 300^0C and (c) 400^0C damage locations, respectively.

To be able to see a notable difference in the speckle images shown in Fig. 3 and 4, it is necessary to look at its 8-bit binary equivalent. To reduce the variables in this work, we only look at a fixed threshold limit for calculating the binary image. Fig. 5 and 6, shows the binary equivalent of the speckle images shown in Fig. 3 and 4, respectively.

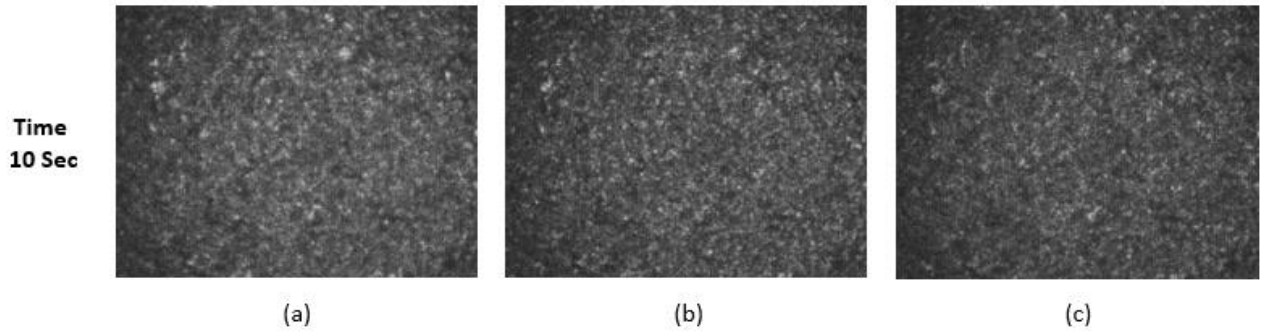

Fig.4 Speckle images captured from the diffuser at 30 seconds into the cooling down cycle of the CFRP at (a) 200^0C, (b) 300^0C and (c) 400^0C

From Fig. 5 and 6, we can easily observe the change in the bulk speckle pattern intensity observed from the diffuser. This could imply that for the defects marked by the locations of 300^0C and 400^0C thermal damage, there could be a higher diffusion of the laser from the surface, a characteristic of surface damages.

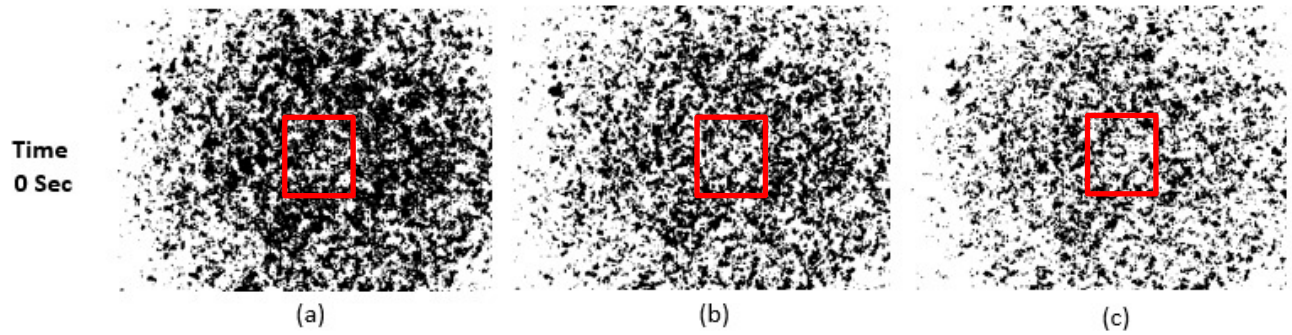

Fig.5 Binary speckle image captured from the diffuser at 0 seconds into the cooling down cycle of the CFRP at (a) 200^0C, (b) 300^0C and (c) 400^0C

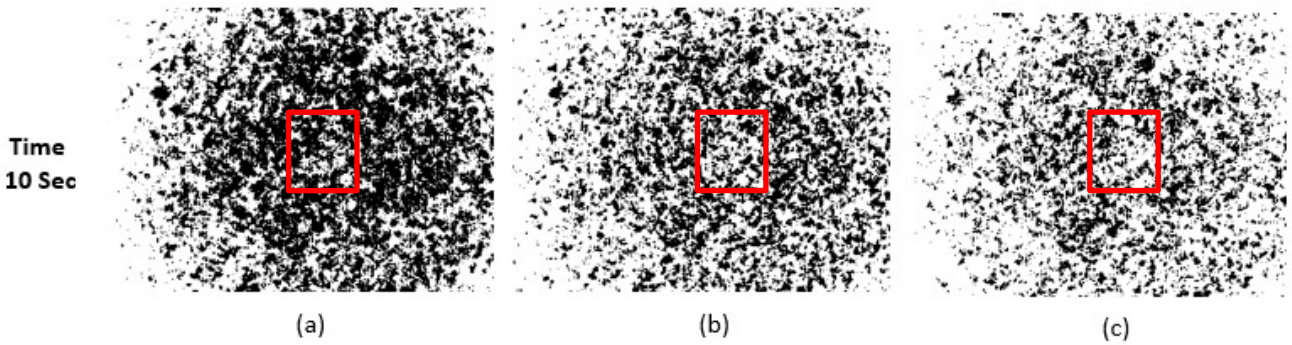

Fig.6 Binary speckle images captured from the diffuser at 30 seconds into the cooling down cycle of the CFRP at (a) 200^0C, (b) 300^0C and (c) 400^0C

From Fig. 5 and 6, it can be observed that there are changes in the speckle pattern through the cooling cycle. For our analysis in this paper, we believe that these changes are a result of mechanical expansions due to the heat excitation. Thermal expansion being a function of the material ambiguities, i.e., the presence of defects or cracks, form an effective method for analyzing the quality of the structure.

In order to estimate whether a change in thermal expansion can be associated with the changes in the speckle pattern, we analyze the transient structure of the speckle pattern observed during the cooling down cycles for each of the locations characterized by the thermal damages.

The focus of the study was also on understanding the fractal property and the element connectivity of the formed speckle pattern. The analysis would compare the specific speckle parameter for each of the individual damaged locations and also its transient variation with the applied thermal excitation.

3.2 Parametric extraction from the speckle images

To characterize the observed speckle patterns, we generate a suitable algorithm in order to obtain specific pattern characteristics, namely, box fractal dimension and the element connectivity.

First, we describe the analysis followed to obtain the box fractal dimension. Fig. 7, shows the variation of transient fractal dimension for the three damage locations, namely, 200^0C, 300^0C and 400^0C.

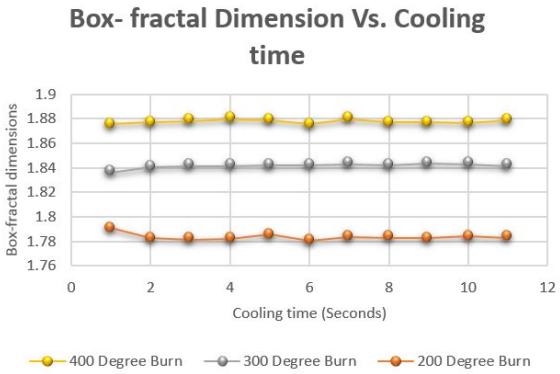

Fig.7 Box-fractal dimension of the transient speckles at three damage locations, 200^0C, 300^0C and 400^0C

We can observe from Fig. 7 that the fractal properties of the speckles observed at the three different locations of thermal damage are different. In fact, the fractal dimension of the area of the specimen affected by 400^0C thermal damage is higher than the areas affected by 300^0C, which itself has a higher fractal dimension compared to the 200^0C thermal damage. This could be a direct implication of surface damage clearly visible for both 300^0C and 400^0C.

It can also be noted that the fractal dimension remains constant with the time of cooling. This implies that the fractal dimension is not a determinantal parameter in understanding the properties of speckles from damaged specimen. We presume that choosing the right camera exposure and setting the adequate threshold limits are essential in understanding the speckle property variations.

In order to better understand the details of the speckle patterns, we also calculate and plot the number of connecting elements in the transient speckle patterns. For a better representation, we distinguish the connectivity by adding a color scale to the images. We represent the component with the maximum connectivity by black while the rest of the components are represented using random RGB. Figures 8 and 9, shows the connecting elements for the binary speckles patterns captured from the diffuser for locations on the panel thermally damaged by (a) 200^0C, (b) 300^0C and (c) 400^0C, at 0 and 10 seconds into the cooling down cycle, respectively.

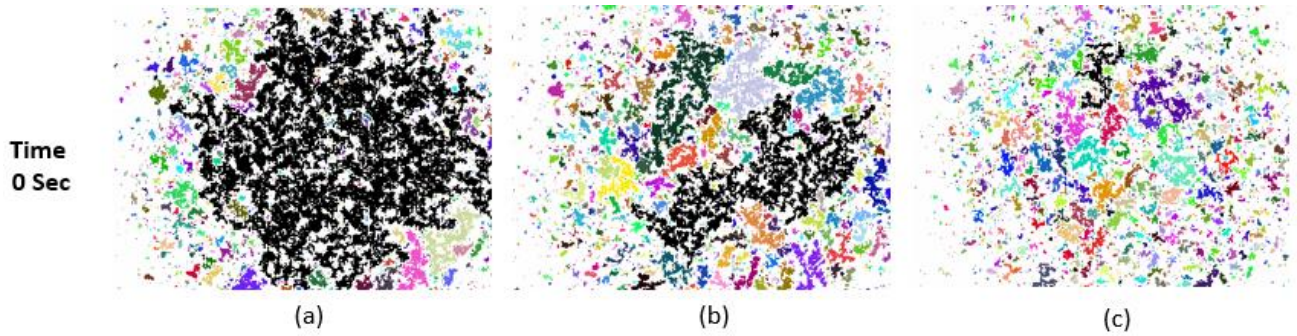

Fig.8 Speckle element connectivity image from the diffuser at 0 seconds into the cooling down cycle of the CFRP at (a) 200^0C, (b) 300^0C and (c) 400^0C

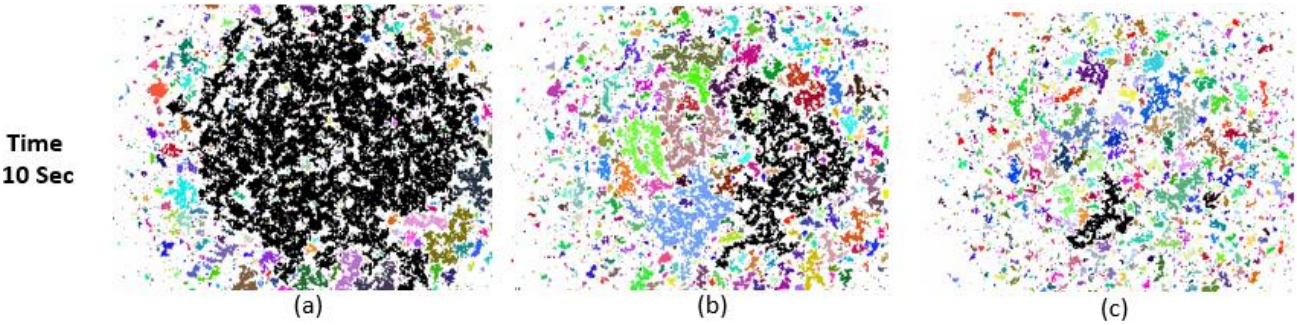

Fig.9 Speckle element connectivity image from the diffuser at 10 seconds into the cooling down cycle of the CFRP at (a) 200^0C, (b) 300^0C and (c) 400^0C

In Fig 8 and 9, the maximum connected elements are shown by the black segments. It can thus be noticed that for the individual damage, the number of connectivity increases with the thermal damage location on the specimen. Thus we notice a notable variation in the transient element connectivity between the three individual damages.

In order to understand the variations in the element connectivity pattern, we use two different methods of transient analysis, namely, the plot of maximum element connectivity (pixels) and the plot of the total number of element connectivities. Fig 10 (a) and (b), describes the transient variation of maximum connectivity and the total number of connectivity for each of the three damaged locations.

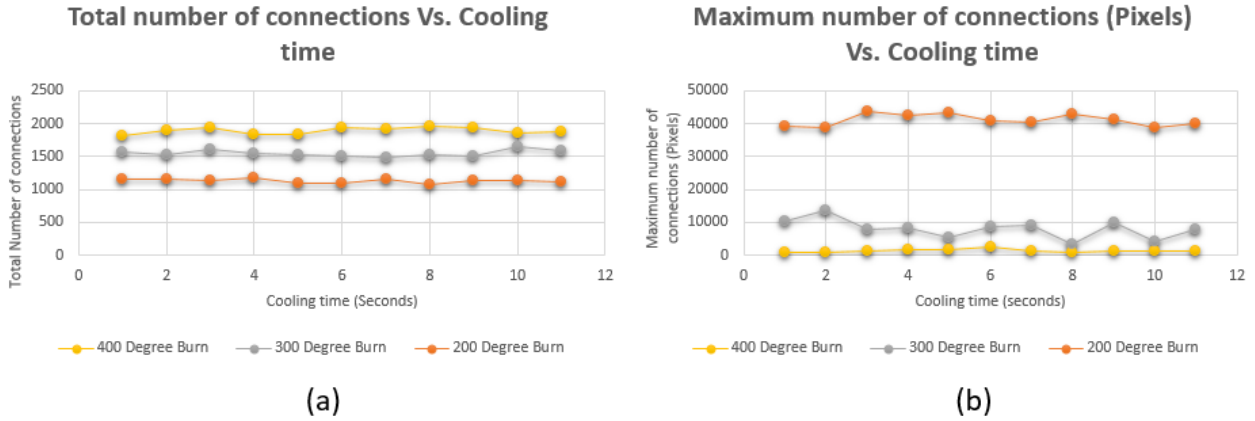

Fig.10 Plots the (a) transient value of the total number of connections for each of the thermally damaged locations and (b) the transient values of the maximum number of connections (pixels).

It can be observed that both the parameters mentioned show a variation with respect to the damage location considered, while there is minimal variation with respect to the cooling time. Particularly, we observe that the total number of connections for the location with the 400^0C damage is higher than the location characterized by 300^0C which itself is higher than the location characterized by the 200^0C damage. Furthermore, an inverse relation is observed with respect to the plot of the variation of the maximum number of element connections with respect to the damage locations. These observations could be a result of surface damage variations of the sample under test. For the sample, we have observed that there is notable surface cracking present on the location characterized by the 400^0C thermal load, lesser when compared to the location thermally damaged by 300^0C (shown in Fig.1 (c)).

Also, there are observably no defects on the location thermally damaged by 200^0C. Thus, for a larger surface damaged segment especially on the locations damaged by the 300^0C and 400^0C thermal loads, we believe that the scatter of the coherent light source introduces a larger number of connecting segments in the speckle pattern while the same scatter reduces the component. Combining our observations from the analysis of the speckle patterns to the inherent surface defects present in the sample, we believe that variations in the parameters characterizing the speckle patterns can lead to the direct representation of the surface damage.

4. CONCLUSIONS

In this paper, a study on the speckle pattern variations from the specimen surface (Shown in 1(b) and 1(c)) due to an external excitation are studied. The specimen in consideration contains multiple thermal damages generated by varying the temperature load. In our previous study, this sample is shown to contains burns and delaminations located on the surface and subsurface, respectively, using shearography and ultrasound inspection techniques. An experimental setup is designed to capture the speckle patterns from the specimen under test after being passed through a diffuser with a fixed grit size. This way, we can compare the variations of the speckle patterns observed from the specimen with more confidence. In order to understand the subsurface damage detection capability, we introduce an external perturbation in the form of heat for the specimen under test. For this, we study the transient variations observed in the speckle pattern during the cooling down cycle at an interval of 3 seconds. Analysis of the observed speckle patterns using two image processing algorithms, namely, fractal analysis and connectivity analysis shows minimal variations in the transient speckle pattern. Rather, the algorithm shows a strong variability with respect to the surface of the specimen under test. Thus, we foresee this developed capability in combination with speckle decorrelation could be an effective method in understanding surface variations, particularly, cracks and corrosion. Advantages of the proposed system enhance the realization of a possible line side speckle image analysis system for surface defect detection. Hence, it is envisaged that this proposed methodology can be applied to in-process industry measurements.

ACKNOWLEDGEMENT

This work was conducted within the Rolls-Royce@NTU Corporate Lab MRT 4.1 project with support from the National Research Foundation (NRF) Singapore under the Corp Lab@University Scheme. The authors are also grateful for the support from COLE EDB funding. One of the authors Aswin Haridas acknowledges the financial support received through NTU under the RSS scheme.

REFERENCES

[1] Edwards T, "Composite Materials Revolutionize Aerospace Engineering," INGENIA, 1, 25-28. (2008).

[2] S. Gholizadeh, "A review of non-destructive testing methods of composite materials," *Procedia Structural Integrity*,1, 50-57 (2016)

[3] V. M. Murukeshan, P. Y. Chan, S. Ong Lin, and A. Asundi, "On-line health monitoring of smart composite structures using fiber polarimetric sensor," *Smart Materials and Structures*, 8(5), 544 (1999).

[4] A. Q. Liu, X. A. Zhang, V. A. Murukeshan, C. Lu, and T. H. Cheng, "Micromachined wavelength tunable laser with an extended feedback model," *IEEE Journal of Selected Topics in Quantum Electronics*, 8(1), 73-79 (2002).

[5] D. J. Whitehouse, "Surface metrology," *Measurement Science and Technology*, 8(9), 955 (1997).
[6] V. M. Murukeshan, and K. V. Sreekanth, "Excitation of gap modes in a metal particle-surface system for sub-30 nm plasmonic lithography," *Optics Letters*, 34(6), 845-847 (2009).
[7] V Sreekanth, K. V.; V. M Murukeshan, J. K Chua, "A planar layer configuration for surface plasmon interference nanoscale lithography," *Applied Physics Letters*, 93(9), 31-34, (2008).
[8] J. W. Goodman, "Some fundamental properties of speckle," *Journal of the Optical Society of America*, 66(11), 1145-1150 (1976).
[9] J. K. Chua, V. M. Murukeshan, S. K. Tan, and Q. Y. Lin, "Four beams evanescent waves interference lithography for patterning of two dimensional features," *Optics Express*, 15(6), 3437-3451 (2007).
[10] K.V Sreekanth, V. M Murukeshan.,"Large-area maskless surface plasmon interference for one- and two-dimensional periodic nanoscale feature patterning" Journal Of The Optical Society Of America A-Optics Image Science And Vision , 27(1), 95-99 (2010).
[11] M.S. Brown and C.B. Arnold, "*Fundamentals of laser-material Interaction and application to multiscale surface modification*," Springer Series in Materials Science 135, Springer-Verlag Berlin Heidelberg, DOI 10.1007/978-3-642-10523-4, 91-120 (2010).
[12] P. Prabhathan, Z. Jing, V. M. Murukeshan, Z. Huijuan, and C. Shiyi, "Discrete and Fine Wavelength Tunable Thermo-Optic WSS for Low Power Consumption C+L Band Tunability," *IEEE Photonics Technology Letters*, 24(2), 152-154 (2012).
[13] U. S. Dinish, Z. X. Chao, L. K. Seah, A. Singh, and V. M. Murukeshan, "Formulation and implementation of a phase-resolved fluorescence technique for latent-fingerprint imaging: theoretical and experimental analysis," *Applied Optics*, 44(3), 297-304 (2005).
[14] E. R. Mendez, and K. A. O'Donnell, "Observation of depolarization and backscattering enhancement in light scattering from gaussian random surfaces," *Optics Communications*, 61(2), 91-95 (1987).
[15] V. M. Murukeshan, J. K. Chua, S. K. Tan, and Q. Y. Lin, "Nano-scale three dimensional surface relief features using single exposure counter-propagating multiple evanescent waves interference phenomenon," *Optics Express*, 16(18), 13857-13870 (2008).
[16] V. K. Shinoj, V. M. Murukeshan, S. B. Tor, N. H. Loh, and S. W. Lye, "Design, fabrication, and characterization of thermoplastic microlenses for fiber-optic probe imaging," *Applied Optics*, 53(6), 1083-1088 (2014).
[17] Francis D. and Tatam R.P, Groves, RM, "Shearography technology and applications: a review," *Measurement science and technology*, 21(10), 1-29 (2010).
[18] R. Sidharthan, and V. M. Murukeshan, "Improved light absorption in thin film solar cell using combination of gap modes and grating back reflector," *Thin Solid Films*, 548(1), 581-584 (2013).
[19] G. Schirripa Spagnolo, and D. Paoletti, "Digital speckle correlation for on-line real-time measurement," Optics Communications, 132 (12), 24-28 (1996).
[20] Y. C. Lam, J. C. Chai, P. Rath, H. Zheng, and V. M. Murukeshan, "A fixed-grid method for chemical etching," International Communications in Heat and Mass Transfer, 31(8), 1123-1131 (2004).
[21] M. Giglio, S. Musazzi, and U. Perini, "Surface roughness measurements by means of speckle wavelength decorrelation," Optics Communications, 28(2), 166-170 (1979).
[22] A. Kishen, V. M. Murukeshan, V. Krishnakumar, and A. Asundi, "Analysis on the nature of thermally induced deformation in human dentine by electronic speckle pattern interferometry (ESPI)," *Journal of Dentistry*, 29(8),531-537 (2001).
[23] P. Lehmann, S. Patzelt, and A. Schöne, "Surface roughness measurement by means of polychromatic speckle elongation," Applied Optics, 36(10), 2188-2197 (1997).
[24] J. W. Goodman, "Dependence of image speckle contrast on surface roughness," Optics Communications, 14(3), 324-327 (1975).
[25] N. K. Krishna Mohan, P. J. Masalkar, V. M. Murukeshan, and R. S. Sirohi, "Separation of the influence of in-plane displacement in multiaperture speckle shear interferometry," *Optical Engineering*, 33(6), 1973-1982 (1994).
[26] G. Schirripa Spagnolo, D. Paoletti, A. Paoletti, and D. Ambrosini, "Roughness measurement by electronic speckle correlation and mechanical profilometry," Measurement, 20(4), 243-249 (1997).
[27] C. J. Tay, S. L. Toh, H. M. Shang, and J. Zhang, "Whole-field determination of surface roughness by speckle correlation," Applied Optics, 34(13), 2324-2335 (1995).

[28] I. Yamaguchi, K. Kobayashi, and L. Yaroslavsky, “Measurement of surface roughness by speckle correlation,” Optical Engineering, 43(11), 2753-2761 (2004).
[29] B. Ruffing, “Application of speckle-correlation methods to surface-roughness measurement: a theoretical study,” Journal of the Optical Society of America A, 3(8), 1297-1304 (1986).
[30] R.D. Correa, J.B. Meireles, J.A.O, Huguenin, D.P. Caetano and L.da Silva, “Fractal structure of digital speckle patterns produced by rough surfaces,” *Physics A*, 392, 869-874 (2013).
[31] Ralph Northdurft, Gang Yao, “Image obscured subsurface inhomogeneity using laser speckle,” *Optics Express*, 13(25), 10034-10039 (2005).
[32] Fu-pen Chiang, “Some new developments in experimental mechanics using random particles and fractal dimensions,” *Proceedings of SPIE*, 4317(1), 1-6 (2001).
[33] Shuai Yuan, Anna Devor, David A. Boas and Andrew K. Dunn, “Determination of optimal exposure time for imaging of blood flow changes with laser speckle contrast imaging,” *Applied Optics*, 44(10), 1823-1830 (2005).
[34] Wong, B.S, Haridas, A., Wei, C. C., "*Ultrasonic and Thermographic Testing of Heat Damaged Composite Materials*". Germany: Lambert Academic Publishing (LAP). ISBN-13: 978-3-659-70982-1, 1-60 (2015).